M(BH3NH2BH2NH2BH3) – the missing link in the mechanism of thermal decomposition of light alkali metal amidoboranes

Journal Name

ARTICLE

M(BH₃NH₂BH₂NH₂BH₃) – the missing link in the mechanism of thermal decomposition of light alkali metal amidoboranes

K. J. Fijalkowski,[a]* T. Jaroń,[a] P. J. Leszczyński,[a] E. Magos-Palasyuk,[b]
T. Palasyuk,[b] M. K. Cyrański[c] and W. Grochala[a]*

We report a novel family of hydrogen–rich materials – alkali metal di(amidoborane)borohydrides, M(BH₃NH₂BH₂NH₂BH₃). The title compounds are related to metal amidoboranes (amidotrihydroborates) but they have higher gravimetric H content. Li salt contains 15.1 wt.% H and it evolves very pure H₂ gas. Differences in thermal stability between amidoboranes and respective oligoamidoboranes allow to explain evolution of ammonia impurity (together with H₂) during thermal decomposition of light alkali amidoboranes, LiNH₂BH₃, NaNH₂BH₃ and NaLi(NH₂BH₃)₂, and confirm the mechanism of the side decomposition reaction.

Introduction

Protonic-hydridic materials (XH_xYH_y) comprise an important family of highly efficient hydrogen stores in the solid state.[1,2] Simultaneous presence of acidic H^+ (attached to a more electronegative element, X) and basic H^- (attached to a more electropositive element, Y) results in low energy barrier and, concomitantly, in low temperature of H_2 desorption from these materials. Systems based on X = nitrogen and Y = boron constitute the most researched protonic–hydridic hydrogen stores.[3,4] These encompass amide–borohydrides,[5,6] NH_4BH_4,[7] ammonia borane (NH_3BH_3)[8,9] as well as its derivatives such as metal amidoboranes, MNH_2BH_3 (MAB phases)[10–21]. Most of these materials suffer from unfavorable thermodynamics, which precludes the re-absorption of H_2 by the discharged residue of the thermal decomposition. Despite emitting impure H_2 gas, the large gravimetric H content (up to 24.4 wt.% for NH_4BH_4) renders them attractive as H storage media for mobile technologies assuming their off-board regeneration.

Here we describe a novel family of hydrogen rich materials –metal di(amidoborane)borohydrides, $M(BH_3NH_2BH_2NH_2BH_3)$ (M(B3N2) phases), as exemplified by lithium and sodium derivatives. The M(B3N2) phases may formally be regarded as derivatives of metal borohydrides, $M[B(H)_2(NH_2BH_3)_2]$ (analogous to the known $M[B(H)_x(CN)_{4-x}]$, $M[B(H)_x(CH_3)_{4-x}]$ or $M[B(H)_x(C_2H_5)_{4-x}]$ salts). The M(B3N2) compounds have much larger gravimetric hydrogen

capacity than MAB phases and they fulfill in excess the DOE gravimetric target in excess [Li(B3N2), 15.1 wt.% H; Na(B3N2), 12.6 wt.% H] which is crucial when designing the storage system (consisting of both: storage material and various mechanical elements) to contain more than 7.5 wt% of hydrogen (Figure 1).

Here we show that the M(B3N2) derivatives constitute the missing link in the mechanism of thermal decomposition of light alkali metal amidoboranes [LiAB, NaAB and NaLi(AB)₂]. On one hand, the transformation of MABs to the corresponding ammonia containing [M(NH₃)](B3N2)] and then formation of M(B3N2) is responsible for the presence of ammonia impurity in the H_2 gas evolved from MABs.[17,22,23] On the other hand, the M(B3N2) salts thermally decompose above 140–160°C and they release more than 50% of their total H content up to 200°C. Importantly, Li salt yields H_2 gas virtually free from any impurities.
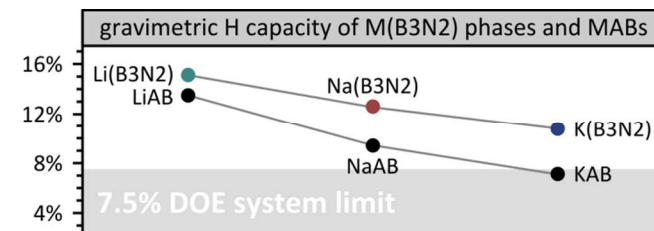

Fig. 1. Comparison of total theoretical hydrogen capacity of light alkali metal M(B3N2) phases and respective amidoboranes, M=Li, Na, K without taking into account weight of other elements of the storage system.
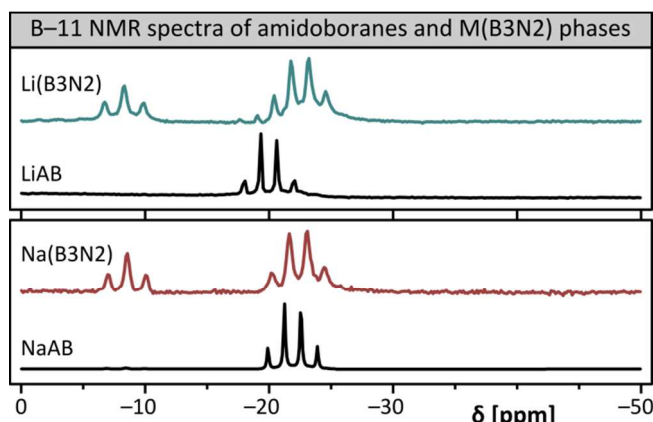
Fig. 2. Comparison of ^{11}B NMR spectra in THF–d$_8$ of M(B3N2) phases (colour lines) and metal amidoboranes (black lines): lithium salts (top) and sodium salts (bottom).

Fig. 3. Comparison of Raman spectra of M(B3N2) phases (colour lines) and metal amidoboranes (black lines): lithium salts (top) and sodium salts (bottom). The NH (3200–3400 cm^{-1}) and BH (1900–2500 cm^{-1}) stretching regions are highlighted.

Results and discussion

The first MB$_x$N$_y$ salt with x > y has probably been synthesized three quarters century ago when Schlesinger and Burg reported in 1938 a light porous solid of a general formula NaB$_2$H$_8$N obtained in reaction of diammoniate of diborane with metallic sodium.[24] The product has been characterized rather incompletely and these results have not been repeated by others. In 2009 two of us have observed evolution of ammonia – along with H$_2$ – during thermal decomposition of alkali metal amidoboranes.[22] Elimination of a volatile nitrogen compound pointed to the formation of a solid residue which was richer in boron as compared to the parent 1:1 stoichiometry of metal amidoboranes. At that time the formation of the "NB$_2$" metal derivatives in the solid state was suggested,[22,23] in accordance with the claim from Schlesinger and Burg.[24]

Probably the first report on Li(B3N2) and Na(B3N2) compound is that in the Ph.D. thesis of Evans in 2011 [25]. The work, however, missed basic characterization data, such as correct stoichiometry and crystal structure, essential for the chemical identity of the compounds. Experimental data contained in PhD thesis of Ryan, 2011[26], although did not present new structural evidence, suggested the formation of a new crystalline compound built of lithium cations and five-membered anionic chains with the following skeleton: BNBNB. The presence of pentameric moieties has recently been suggested for sodium compound by W. C. Ewing *et al.*[27], 2013. The reported ^{11}B NMR spectrum revealed the presence of (BH$_2$)$_1$(BH$_3$)$_2$ constituents of the anions. The authors, however, did not present any data on crystal structure of the studied material.

We have now conducted a systematic study of the two lightest alkali metal M(B3N2) phases, M = Li, Na using ^{11}B NMR, single- and powder X-ray diffraction, IR absorption, Raman scattering, thermogravimetry and differential scanning calorimetry. We have been able to solve the crystal structures of the M(B3N2) phases, M = Li, Na and provide complete physicochemical characterization in relation to hydrogen storage properties. Comparative analysis of the M(B3N2) phases with their MABs analogues has been also carried out.

M(B3N2) phases were conveniently obtained in reaction of ammonia borane with respective metal hydride in molar ratio 3:1 in anhydrous THF (see ESI):
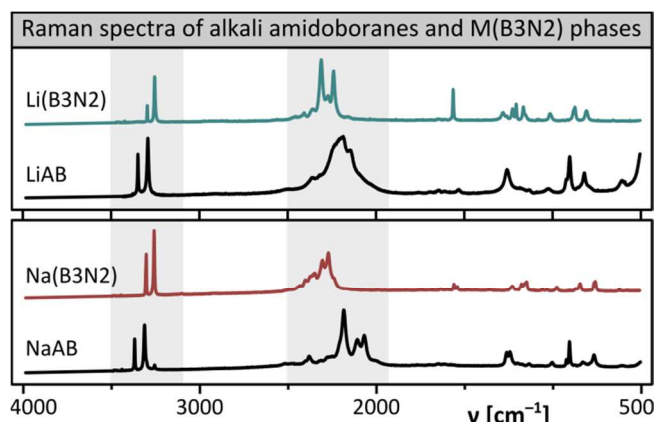
$$MH + 3NH_3BH_3 \rightarrow M(BH_3NH_2BH_2NH_2BH_3) + NH_3\uparrow + 2H_2\uparrow$$

Mechanochemical synthesis followed by thermal desorption of excess NH$_3$ is an alternative approach [24] (ESI).

Alkali metal M(B3N2) phases are white low-density solids which are sensitive to moisture. Li(B3N2) and Na(B3N2) are stable at room temperature in contrast to respective MABs,[23] as discussed below. Li(B3N2) is well soluble in THF in contrary to Na(B3N2). Nevertheless, solubility of both compounds is sufficient to obtain the ^{11}B NMR spectra (Figure 2). The spectra are different from those of the respective metal amidoboranes (SI) and they reveal the presence of a characteristic quarter at *ca.* −21 ppm representing [BH$_3$] groups and a twice weaker triplet at *ca.* −8 ppm representing [BH$_2$] moieties, thus confirming the presence of the (BH$_2$)$_1$(BH$_3$)$_2$ constituents of the anions. The spectra also confirm the presence of small amount of LiAB impurity in the sample of Li(B3N2).

All alkali metal M(B3N2) phases are characterized by similar and characteristic Raman (Figure 3) and FTIR spectra (SI) which are easily distinguishable from the spectra of respective metal amidoboranes (MABs). In general, the sharp doublet in the Raman spectra assigned to the symmetric NH stretching modes appears at smaller wavenumbers for M(B3N2) phases than for the respective MABs. Simultaneously, the most intense BH stretching bands fall at higher wavenumbers for M(B3N2) phases than for the respective MABs. These features suggest that the N–H bonds are somewhat weaker for M(B3N2) phases than for MABs, while the opposite holds true for the B–H bonds. While the stiffening of the B–H modes is in qualitative agreement with the trend predicted from our DFT calculations for the isolated (NH$_2$BH$_3$)$^-$ and (BH$_3$NH$_2$BH$_2$NH$_2$BH$_3$)$^-$ anions in the gas phase, the softening of the N–H bonds observed in experiment is in disagreement with the computed trend (SI), and it likely originates from the solid state effects (differences of packing, interactions of anions with cations, or secondary interactions such as possible dihydrogen bonding, etc.).

One sharp band coming from the HNH bending vibration at 1571 cm^{-1} is seen in the Raman spectrum of Li(B3N2); the presence of a single band suggests that the NH$_2$ groups have identical local symmetry (hence only the in-phase HNH bending is Raman-active). Indeed, as we will see below, the (BH$_3$NH$_2$BH$_2$NH$_2$BH$_3$)$^-$ moiety in the crystal structure of Li(B3N2) is found in the *n*-alkane-like quasi-linear geometry with two crystallographically equivalent NH$_2$ units.

The samples of alkali metal M(B3N2) phases were studied with powder x-ray diffraction (PXD) (Figure 4).
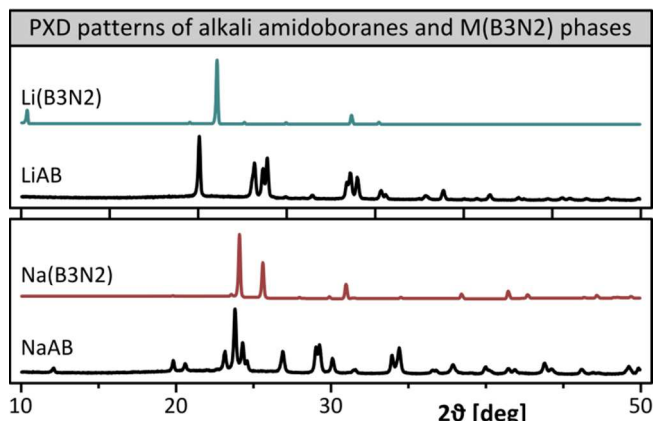
Fig. 4. Comparison of PXD patterns of M(B3N2) phases (colour lines) and respective amidoboranes (black lines): lithium (top) and sodium salts (bottom).

Table 1. Comparison of lattice parameters for three alkali metal M(B3N2) phases.

Compound	System	Space Group	a [Å]	c [Å]	V [Å^3]	Z
Li(B3N2) [a]	Tetragonal	$P\text{–}42c$	4.02(1)	16.95(5)	273.9 (12)	2
Na(B3N2) [b]	Hexagonal	$P6_3/m$	4.3392(2)	17.853(6)	291.11(18)	2

[a] Compare Ref.[25,26]; [b] Compare Ref.[25].

Lattice parameters of Li(B3N2) determined in this work are in accordance with the values obtained for the compounds reported by Evans[25] and by Ryan[26] (Table 1 and SI). This result suggests that chemical identity of all three crystalline samples may be the same even though Evans suggested a different stoichiometry for this compound. Evans proposed chemical formula of $Li(NH_3)^+(BH_3NH_2BH_3)^-$ containing ammonia molecule weakly bound to alkali metal cation[24]. Results of our spectroscopic measurements (Raman or IR), however, did not reveal any significant bands in the 3350–3400 cm^{-1} region, characteristic for $Li(NH_3)^+$ cations.[17] Moreover, we observed that Li(B3N2) evolves pure hydrogen on heating (see below), which corroborate the absence of the $Li(NH_3)^+$ cation in material. Based on a combination of NMR, FTIR, and Raman spectra, as well as PXD we have been able to confirm the stoichiometry of $Li(BH_3NH_2BH_2NH_2BH_3)$ which was previously suggested by Ryan.[25] The crystal structure of Li(B3N2) consists of Li$^+$ layers which are linked via five member chain $(BH_3NH_2BH_2NH_2BH_3)^-$ anions which coordinate lithium cations using hydrogen atoms of terminal [BH$_3$] groups only (Figure 5). Recall, the N atoms of the $(BH_3NH_2BH_2NH_2BH_3)^-$ anions do not have any lone pairs available for coordination to metal centers, hence only the basic hydride anions at boron may be used for bonding. Lithium cations are found in tetrahedral coordination of four hydrogen atoms, resembling that found for the orthorhombic form of LiBH$_4$ and is different from the first coordination sphere of Li in LiAB (the N$_1$H$_4$ coordination). The shortest Li–H distance is 2.0(2) Å (as compared with the corresponding distance of 1.98(1) Å in Pbca LiAB[28] and the one of 1.98(1) Å in Pnma LiBH$_4$[29]). The average B–N bond length of the $(BH_3NH_2BH_2NH_2BH_3)^-$ anion is *ca* 1.59(6) Å (as compared with 1.55 Å for LiAB[10]) while the average angles between the B–N bonds (115°) are close to the tetrahedral angle. The crystal structure contain disordered $(BH_3NH_2BH_2NH_2BH_3)^-$ anions lying along the z axis of the unit cell. Importantly, the inter-anion dihydrogen bonds are absent from the crystal structure of Li(B3N2).
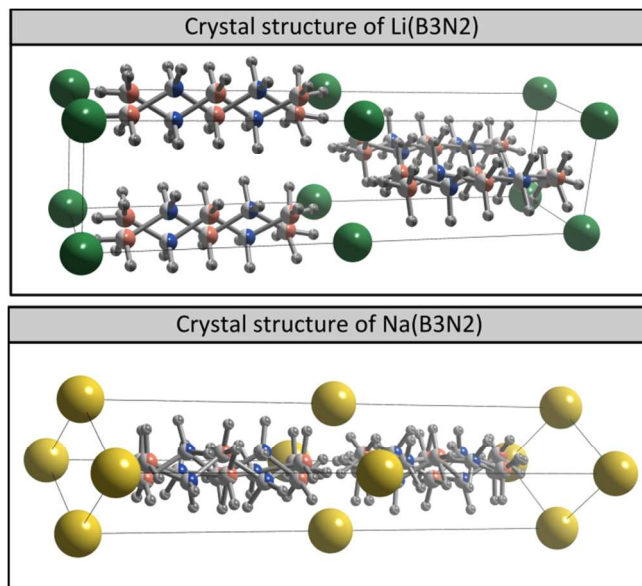

Fig. 5. Crystal structure of alkali metal M(B3N2) phases as determined with PXD: H grey, B red, N blue, Li green, Na yellow. Li(B3N2) – top, Na(B3N2) – bottom. Crystallographic positions with partial population are marked with partly–colored balls.

The volume of Li(B3N2) per one formula unit, 136.95(6) Å^3, is smaller by only 3.3 % than the expected volume of this compound (141.65 Å^3), which may be derived from the following equation:

$$V[Li(BH_3NH_2BH_2NH_2BH_3)] = \\ = 3V[Li(NH_2BH_3)] - V[LiNH_2] - V[LiH] \quad (2)$$

The PXD for Na(B3N2) yields a diffraction pattern which can be indexed using the trigonal cell proposed by Evans.[25] We have determined the crystal structure of Na(B3N2) in a centrosymmetric primitive hexagonal $P6_3/m$ cell with Z = 2 (Table 1 and SI). There are three important similarities between crystal structures of Na(B3N2) and Li(B3N2). First, Na(B3N2) also consists of metal cation layers separated by layers containing the $(BH_3NH_2BH_2NH_2BH_3)^-$ anions. Second, the anions are substantially disordered along the z axis. Third, metal cations are found in homoleptic environment of hydrogen atoms of the terminal [BH$_3$] groups. In consequence, sodium cations exhibit a coordination with 8 H atoms (=12 • ⅔) and the closest Na–H distance of 2.22(9) Å. This may be compared to the shortest Na–H separation of *ca*. 2.33 Å seen for NaAB (*cf.* SI) and a much larger value of *ca*. 2.58 Å typical of the disordered room-temperature rocksalt form of NaBH$_4$.[30] Obviously, the metal-hydrogen bond lengths listed here for both M(B3N2) salts should be given only limited trust due to inherent problems related with solving disordered crystal structures of compounds built of low-Z elements using laboratory x-ray radiation source.[31]

The density functional theory as well as the Møller-Plesset perturbation theory calculations for the isolated $(BH_3NH_2BH_2NH_2BH_3)^-$ anion in the gas phase (Figure 6) indicate, that the C$_{2v}$ form is somewhat less stable than the C$_1$ form. The relative energy of the C$_1$ isomer with respect to the C$_{2v}$ one (corrected for energy of zero-point vibrations) is around –0.15 eV ± 0.01 eV. However, since the energy difference is not very large, it may be anticipated that the interactions of anions with cations as well as the differences of packing, lead to the small preference of the C$_{2v}$ quasi-alkane

form in the solid state.[32] These calculations also show that the hydride anions of the terminal BH_3 groups are most basic (*i.e.* negatively charged) H atoms of the anion, which provides further confirmation of their capability to coordinate metal cations. Note that the B–N bond lengths of the C_{2v} form are close to the experimentally determined value of 1.59(6) Å.
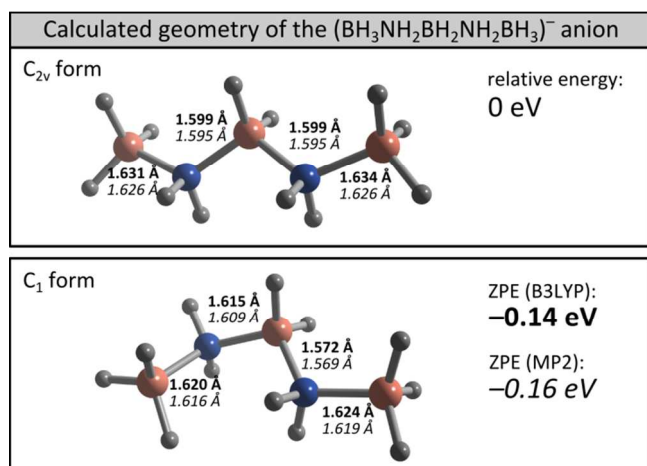

Fig. 6. The calculated geometry of the $(BH_3NH_2BH_2NH_2BH_3)^-$ anion in the C_{2v} form (top) and C_1 form (bottom) as optimized at the 6–311++G**/B3LYP (bold) or /MP2 (italics) level of theory. Zero-point vibrational energy-corrected relative energy in eV.
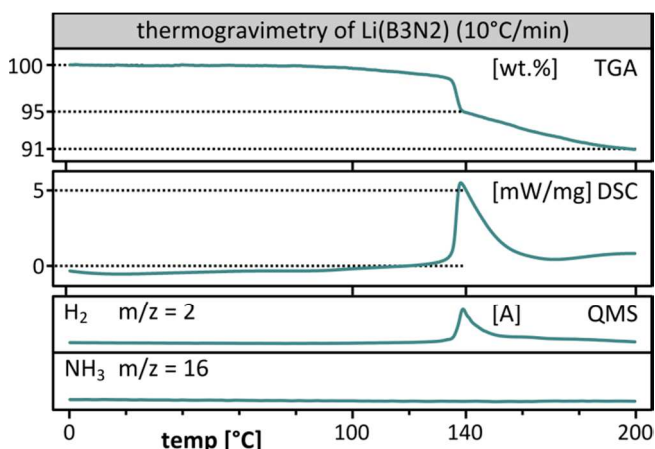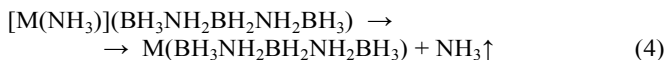

Fig. 7. The TGA/DSC profiles and well as the ion current for m/z = 2 (H_2) and 16 (NH_3) measured for thermal decomposition of Li(B3N2), 10 K/min scanning rate.

We have investigated thermal stability of alkali M(B3N2) phases under inert argon atmosphere (at –35°C, at room temperature and upon heating to 200°C, Figure 7) in comparison to those of respective amidoboranes. Recall, LiAB, NaAB and NaLi(AB)$_2$ are unstable at room temperature and they decompose spontaneously while releasing hydrogen contaminated by ammonia.[17,22,23] After several days of storing sample of light alkali amidoboranes at RT they are contaminated with the traces of M(B3N2) phases (for PXD patterns see SI). Contamination of LiAB and NaAB samples by traces of Li(B3N2) and Na(B3N2) may be observed in PXD patterns reported in our previous reports[17,33] and independently by other groups [10,26,34] (SI). Furthermore, heating of light alkali amidoborane samples to *ca.* 50°C drives an accelerated formation of respective M(B3N2) phases (which can be detected by PXD) accompanied by the evolution of ammonia (Figure 8):

$$3M(NH_2BH_3) \rightarrow [M(NH_3)](BH_3NH_2BH_2NH_2BH_3) + 2[M] \quad (3)$$

$$[M(NH_3)](BH_3NH_2BH_2NH_2BH_3) \rightarrow$$
$$\rightarrow M(BH_3NH_2BH_2NH_2BH_3) + NH_3\uparrow \quad (4)$$

where [M] in Eq.(3) stands for unbalanced alkali metal, while indicating that that the true pathway of the decomposition reaction is more complex than the one proposed here. One possibility to balance Eq.(3) is that of formation of amorphous $M_2(NHBH_3)$ phases:

$$5 M(NH_2BH_3) \rightarrow [M(NH_3)](BH_3NH_2BH_2NH_2BH_3) +$$
$$+ M_2(NHBH_3) + H_2\uparrow \quad (5)$$
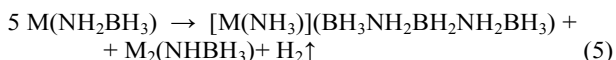
However, we choose not to speculate further about the mechanism of the side reaction due to largely amorphous nature of the products as well as insufficient amount of experimental data.
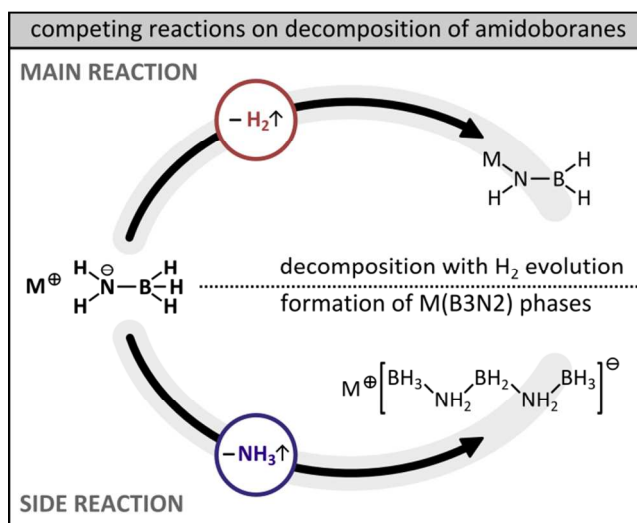

Fig. 8. The simplified mechanism of two competing reactions during thermal decomposition of alkali metal amidoboranes: direct evolution of H_2 (top) and formation of M(B3N2) phases with evolution of NH_3 (bottom).

Li(B3N2) and Na(B3N2) salts are much more thermally stable than their amidoborane analogues; they decompose exothermally at temperatures over 140–160°C (Figure 7 and SI).[19] Crystalline $LiBH_4$ and $NaBH_4$ were identified in the solid residues of dehydrogenation of the respective M(B3N2) phases, suggesting the following tentative mechanism of the thermal decomposition :[17]

$$M(BH_3NH_2BH_2NH_2BH_3) \rightarrow MBH_4 + 2/n\ (NHBH)_n + 2\ H_2\uparrow \ (6)$$

The expected mass loss according to Eq.(5) is 5.0% (for Li salt). The first sudden mass loss observed for the Li sample at 140°C is *ca.* 5 wt.%, in a crude agreement with the simplified mechanism described by Eq.(6). Additional mass loss is observed for temperatures of up to 200°C which suggests that the resulting $(NHBH)_n$ also decomposes to some extent while releasing H_2:

$$1/n\ (NHBH)_n \rightarrow BN + H_2\uparrow \quad (7)$$

Importantly, Li(B3N2) releases very pure H_2 gas, free from ammonia and any other N-B-H impurities. This feature (together with the increased total H content) represents a major advantage of Li(B3N2) phases over the pristine LiAB, which yields hydrogen severely polluted with ammonia.[22,35]
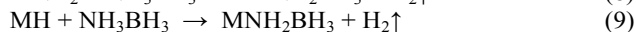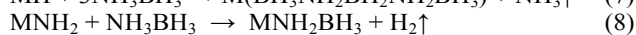
Conclusions

We have synthesized and characterized two novel protonic–hydridic compounds, the lithium and sodium M(B3N2) derivatives containing the $(BH_3NH_2BH_2NH_2BH_3)^-$ anions. These lightweight salts constitute novel H–rich materials of high gravimetric and volumetric hydrogen capacity (12.6–15.1 wt.% H); they are stable at room temperature. Li salt releases pure H_2 gas upon heating in the 140–200°C temperature range, which is of immense importance for practical applications. This - together with the increased total H content - represents a major advantage of Li(B3N2) phases over the pristine LiAB, which yields H_2 severely polluted with ammonia.[22,39] Metal borohydrides constitute the only crystalline products of their thermal decomposition of the M(B3N2) salts.

The spontaneous formation of M(B3N2) phases in the samples of LiAB, NaAB and NaLi(AB)$_2$ at room temperature changes the N:B balance of the solids from 1:1 to ⅔:1 which is responsible for the evolution of ammonia impurity (along with H_2) from pristine MAB salts. The exact mechanism of formation of the M(B3N2) phases as a side reaction taking place during thermal decomposition of MAB phases, is currently unknown. One of the supposed scenarios may involve the short-lived intermediates containing related but shorter B2N backbone, and similar to NaB_2H_8N reported in 1930's,[24] but more experimental evidence is needed to confirm it.

Experimental

Synthetic procedures Alkali metal M(B3N2) phases and amidoboranes were synthesized in direct reaction of alkali metal hydride with ammonia borane in dry THF in the argon gas atmosphere. We have used reagents of the highest commercially available purity: LiH, LiNH$_2$ NaH (95%, Sigma Aldrich) and NH_3BH_3 (98%, JSC Aviabor). THF (99.9%, Sigma Aldrich) was firstly dried over yttrium borohydride or sodium hydride and then distilled.

We have performed synthesis of M(B3N2) phases (Eq. 7) and amidoboranes (Eqs. 8, 9) according to the following reaction equations:

$$MH + 3NH_3BH_3 \rightarrow M(BH_3NH_2BH_2NH_2BH_3) + NH_3\uparrow \quad (7)$$
$$MNH_2 + NH_3BH_3 \rightarrow MNH_2BH_3 + H_2\uparrow \quad (8)$$
$$MH + NH_3BH_3 \rightarrow MNH_2BH_3 + H_2\uparrow \quad (9)$$

Reactions were performed in THF solution at room temperature with continuous stirring for 24h or in a disc mill in mechanosynthetic metod. The solid products were washed several times with fresh portions of THF and left to dry; they were analyzed without further purification. Samples were stored under argon atmosphere in Labmaster DP MBRAUN glovebox (O_2 < 1.0 ppm; H_2O < 1.0 ppm) at −35°C. All further analyses were performed under inert atmosphere or in vacuum.)

Thermal decomposition was investigated using an STA 409 simultaneous thermal analyzer from Netzsch, in the temperature range −10°C to +350°C. STA 409 allows for simultaneous thermogravimetric analysis (TGA), differential scanning calorimetry (DSC) and evolved gas analysis (QMS). The samples were loaded into alumina crucibles. High purity 6N argon was used as a carrier gas. The evolved gases were analyzed with a QMS 403C Aëolos mass spectrometer from Pfeiffer–Vacuum. Transfer line was preheated to 200°C to avoid condensation of residues.

Infrared absorption spectroscopy: All substrates, products and thermally decomposed samples were characterized with infrared absorption spectroscopy in KBr pellets using a Vertex 80v vacuum FT–IR spectrometer from Bruker. The samples sealed in a 0.6 mm thick quartz capillary under Ar were also characterized by Raman spectroscopy using Custom designed setup for micro Raman based on monochromator Jobin Yvon THR1000 with CCD detection. Excitation line 632.8 nm was used.

Powder X-ray diffraction: PXD patterns of solids (sealed under argon inside 0.6 mm thick quartz capillaries) were measured using two diffractometers: a) Panalytical X'Pert Pro diffractometer with linear PIXcel Medipix2 detector (parallel beam; the CoK$_{\alpha1}$ and CoK$_{\alpha2}$ radiation intensity ratio of *ca.* 2:1, $\lambda \sim 1.789$ Å), denoted here as CoK$_\alpha$; b) Bruker D8 Discover diffractometer with 2D Vantec detector (parallel beam; the CuK$_{\alpha1}$ and CuK$_{\alpha2}$ radiation intensity ratio of *ca.* 2:1, $\lambda \sim 1.5406$ Å), denoted here as CuK$_\alpha$. All PXD results are shown in copper scale.

The diffraction signals of M(B3N2) phases, M=Li,Na, were indexed using X-cell program[36] (Accelrys). Due to significant disorder and presence of peaks from unidentified impurities the successful structure solution was only possible after proper identification of the anions from spectroscopic methods (M=Li,Na) and information on the BNBNB backbone from the single crystal diffraction (M=Na). In both cases the structure solution was attempted in several unit cells using a real-space method implemented in program FOX[37]. Finally, as the unit cells of lower symmetry did not lead to significant improvement of fit, we have chosen the high-symmetry solutions which reproduced the experimental patterns very well and refined the starting models in Jana2006[38]. Several restraints were necessary to remain the realistic geometry of the anions: for M=Li,Na; all the N–H and B–H distances and angles related to hydrogen atoms were restrained to 1.10(1) Å, and 109.5(5)° (M=Li) or 109.47(5)° (M=Na), respectively; for M=Na also B–N distances were restrained to 1.60(1) Å; the atomic displacement parameters (ADP) of H atoms were set as 1.2–1.5 of ADP of adjacent heavier atom. Weak scattering of X-ray by hydrogen atoms allows for only rough determination of their positions, therefore all the distances involving hydrogen atoms should be treated as approximate approach. The pseudo-Voigt peak shape function was used; the background has been modeled manually. Further details of the crystal structure investigation(s) may be obtained from the Fachinformationszentrum Karlsruhe, 76344 Eggenstein-Leopoldshafen (Germany), on quoting the depository number CSD numbers: 428007 – Li($B_3N_2H_{12}$), 428008 – Na($B_3N_2H_{12}$).

^{11}B NMR spectra of M(B3N2) phases and respective amidoboranes were obtained using a NMR UnityPlus 200 MHz VARIAN spectrometer with BF_3:C_2H_5–O–C_2H_5 as an external standard and 1H NMR measurements with TMS. THFd$_8$ (Aldrich, 99.5 atom% D), dried over metallic sodium, was used as a solvent.

Acknowledgements

Notes and references

[a] Center of New Technologies, University of Warsaw, ul. Zwirki i Wigury 93, 02-089 Warsaw, POLAND.

[b] Institute of Physical Chemistry, Polish Academy of Sciences, ul. Kasprzaka 44/52, 01-224 Warsaw, POLAND.

[c] Faculty of Chemistry, University of Warsaw, ul. Pasteura 1, 02-093 Warsaw, POLAND.

† Footnotes should appear here. These might include comments relevant to but not central to the matter under discussion, limited experimental and spectral data, and crystallographic data.

Electronic Supplementary Information (ESI) available: [details of any supplementary information available should be included here]. See DOI: 10.1039/b000000x/

1   W. Grochala, P. P. Edwards, *Chem. Rev.*, 2004, **104**, 1283.
2   Ł. Maj, W. Grochala, *Adv. Funct. Mater.*, 2006, **16**, 2061.
3   C. W. Hamilton, R. T. Baker, A. Staubitzc, I. Manners, *Chem. Soc. Rev.*, 2009, **38**, 279.
4   A. J. Churchard, E. Banach, A. Borgschulte, R. Caputo, J.-C. Chen, D. Clary, K. J. Fijalkowski, H. Geerlings, R. V. Genova, W. Grochala, T. Jaron, J. C. Juanes-Marcos, B. Kasemo, G. J. Kroes, I. Ljubic, N. Naujok, J. K. Norskov, R. A. Olsen, F. Pendolino, A. Remhof, L. Romanszki, A. Tekin, T. Vegge, M. Zach, A. Zuttel, *Phys. Chem. Chem. Phys.*, 2011, **13**, 16955.
5   F. E. Pinkerton, G. Meisner, M. Meyer, M. Balogh, M. J. Kundrat, *Phys. Chem. B*, 2005, **109**, 6.
6   Z. Xiong, G. Wu, J. Hu, P. Chen, *Adv. Mater.* 2004, **16**, 1522.
7   R. W. Parry, D. R. Schultz, P. R. Girardot, *J. Am. Chem. Soc.*, 1958, **80**, 1.
8   S. G. Shore, R. W. Parry, *J. Am. Chem. Soc.*, 1955, **77**, 6084-6085.
9   J. Baumann, E. Baitalow, G. Wolf, *Thermochim. Acta*, 2005, **430**, 9.
10 Z. Xiong, C. K. Yong, G. Wu, P. Chen, W. Shaw, A. Karkamkar, T. Autrey, M. O. Jones, S. R. Johnson, P. P. Edwards, W. I. F. David, *Nature Mater.*, 2008, **7**, 138.
11 H. V. K. Diyabalanage, T. Nakagawa, R. P. Shrestha, T. A. Semelsberger, B. L. Davis, B. L. Scott, A. K. Burrell, W. I. F. David, K. R. Ryan, M. Owen Jones, P. P. Edwards, *J. Am. Chem. Soc.*, 2010, **132**, 11836.
12 J. Luo, X. Kang, P. Wang, *Energy Environ. Sci.*, 2012, **6**, 1018-1025
13 H. V. K. Diyabalanage, R. P. Shrestha, T. A. Semelsberger, B. L. Scott, M. E. Bowden, B. L. Davis, A. K. Burrell, *Angew. Chem. Int. Ed.*, 2007, **46**, 8995.
14 J. Spielmann, G. Jansen, H. Bandmann, S. Harder, *Angew. Chem. Int. Ed.*, 2008, **47**, 6290.
15 Q. Zhang, Ch. Tang, Ch. Fang, F. Fang, D. Sun, L. Ouyang, M. Zhu, *J. Phys. Chem. C*, 2010, **114**, 1709.
16 R. V. Genova, K. J. Fijalkowski, A. Budzianowski, W. Grochala, *J Alloys Comp.*, 2010, **499**, 144.
17 K. J. Fijalkowski, R. V. Genova, Y. Filinchuk, A. Budzianowski, M. Derzsi, T. Jaroń, P. Leszczyński, W. Grochala, *Dalton Trans.*, 2011, **40**, 4407.
18 Y. Zhang, K. Shimoda, T. Ichikawa, Y. Kojima, *J. Phys. Chem.*, 2010, **114**, 14662.
19 W. Li, L. Miao, R. H. Scheicher, Z. Xiong, G. Wu, C. M. Araujo, A. Blomqvist, R. Ahuja, Y. Feng, P. Chen, *Dalton Trans.* 2012, **41**, 4754.
20 X. Kang, J. Luo, Q. Zhang, P. Wang, *Dalton Trans.*, 2011, **40**, 3799.
21 H. Wu, W. Zhou, F. E. Pinkerton, M. S. Meyer, Q. Yao, S. Gadipelli, T. J. Udovic, T. Yildirim, J. J. Rush, *Chem. Comm.*, 2011, **47**, 4102.
22 K. J. Fijalkowski , W. Grochala, *J. Mater. Chem.*, 2009, **19**, 2043.
23 K. J. Fijalkowski, R. Jurczakowski, W. Kozminski, W. Grochala, *Phys. Chem. Chem. Phys.*, 2012, **14**, 5778.
24 H. I. Schlesinger, A. B. Burg, *J. Am. Chem. Soc.*, 1938, **60**, 290.
25 I. C. Evans, PhD dissertation, University of Birmingham, 2011.
26 K. R. Ryan, PhD dissertation, University of Oxford, 2011.
27 W. C. Ewing , P. J. Carroll , L. G. Sneddon, *Inorg. Chem.*, 2013, **52**, 10690.
28 H. Wu, W. Zhou, T. Yildirim, *J. Am. Chem. Soc.*, 2008, **130**, 14834.
29 J-Ph. Soulié, G. Renaudin, R. Černý, K. Yvon, *J. Alloys. Compd.*, 2002, **346**, 200.
30 R. S. Kumar, A. L. Cornelius, *Appl. Phys. Lett.*, 2005, **87**, 261915, 1.
31 Crystallographic density of both M(B3N2) salts is quite low, about 0.96 g cm^{-3} for M = Li and 1.09 g cm^{-3} for M = Na, but in the range typical for H-rich salts of these metals.
32 The Rietveld fit of the crystal structure of Na(B3N2) is of somewhat poorer quality than that for its lithium analogue. It could be that the presence of a fraction of the C_1-like anionic moieties in the crystal structure model would improve fit parameters. We have not tried this due to generally weak diffraction from this sample.
33 E.g., in our paper on NaLi(AB)$_2$ we have noticed an unknown impurity that we denoted as "*P*1 phase" (Ref.[17]) which has now been identified as Na(B3N2).
34 C. Wu, G. Wu, Z. Xiong, W. I. F. David, K. R. Ryan, M. O. Jones, P. P. Edwards, H. Chu, Chen, *Inorg. Chem.*, 2010, **49**, 4319.
35 *Cf.*: Y. S. Chua, P. Chen, G. Wu, Z. Xiong, *Chem. Commun.* 2011, **47**, 5116, and references therein
36 M. A. Neumann, *J. Appl. Cryst.*, 2003, **36**, 356.
37 V. Favre-Nicolin, R. Černý, *J. Appl. Cryst.*, 2002, **35**, 734.
38 V. Petricek, M. Dusek, L. Palatinus, *Jana2006. Structure Determination Software Programs. Institute of Physics*, Praha, Czech Republic, 2006.